

Hydrogen-induced Sb atom reconstruction $\sqrt{3} \times \sqrt{3} \rightarrow 2 \times 1$ on Si(111) as an example of a six-state model

V. Petrauskas and E. E. Tornau

Semiconductor Physics Institute, Goštauto 11, LT-01108 Vilnius, Lithuania

(Received 21 September 2006; revised manuscript received 1 December 2006; published 14 March 2007)

A six-state model is proposed to describe the hydrogen-induced $\sqrt{3} \times \sqrt{3}$ (trimers) $\rightarrow 2 \times 1$ (zigzag chains) reconstruction of 1 ML of Sb atoms on Si(111). Attractive nearest-neighbor Sb-Sb pair interactions and also triple interaction v_t are considered. The phase diagram of the system with and without v_t is calculated when no hydrogen atoms are adsorbed. Second-order phase transitions are obtained between a disordered phase and both ordered phases, $\sqrt{3} \times \sqrt{3}$ and 2×1 , when $v_t=0$. The possibility of phase separation close to the $\sqrt{3} \times \sqrt{3} \rightarrow 2 \times 1$ phase boundary is discussed when v_t interaction is included. Corroborating recent experimental data, we demonstrate that adsorption of small coverage of hydrogen atoms turns the $\sqrt{3} \times \sqrt{3}$ phase into mixed $\sqrt{3} \times \sqrt{3}$ and 2×1 structure. The length and number of zigzag chains grow with the increase in hydrogen concentration.

DOI: 10.1103/PhysRevB.75.113308

PACS number(s): 68.35.Rh, 64.60.Cn, 68.47.Fg

A monolayer (ML) coverage by group-V atoms on Si(111) or Si(001) surfaces turns the growth mode of Ge on Si from the usual three-dimensional (3D) Stranski-Krastanov growth to that of the layer by layer. Therefore, Si(111) surfaces covered by As, Sb, and Bi are intensively studied in search of the optimal surfactants for Ge epitaxy on Si.

At Sb saturation coverage of 1 ML, the domains of three Sb-formed reconstructions have been observed on Si(111) surface: $\sqrt{3} \times \sqrt{3}$,¹⁻⁵ 2×1 ,⁶ and 1×1 .⁵ Usually, one of these phases and patches of accompanying phases are obtained depending on preparation conditions—initial Sb coverage, its flux rate, and substrate temperature. Evaporation of 3 ML of Sb at 650–670 °C and further desorption lead to formation of 1 ML $\sqrt{3} \times \sqrt{3}$ -Sb/Si(111) structure;³⁻⁵ room-temperature adsorption at very low Sb flux rates is favorable for the occurrence of 1×1 structure;⁵ deposition at room temperature and subsequent annealing at 630 °C result in 2×1 -Sb/Si(111) reconstruction with patches of 1×1 and $\sqrt{3} \times \sqrt{3}$ phases.⁶

As demonstrated by scanning tunneling microscopy (STM) experiments⁴ and first-principles *ab initio* calculations,^{3,7-9} in all ordered Sb/Si(111) structures, Sb atoms prefer the positions on top of the first layer Si atom. However, in both $\sqrt{3} \times \sqrt{3}$ and 2×1 structures, Sb atoms are slightly shifted from the ideal top position, as shown in Fig. 1. In $\sqrt{3} \times \sqrt{3}$, three neighboring Sb atoms move toward the mutual center on top of the second layer Si atom in the so-called T_4 site and form trimers (milk-stool model). In the 2×1 phase, Sb atoms form zigzag chains.

Regarding other similar systems at 1 ML coverage, it is known that the milk-stool T_4 - $\sqrt{3} \times \sqrt{3}$ arrangement is characteristic of Bi/Si(111).¹⁰⁻¹² In turn, for Sb/Ge(111) the 2×1 phase was found experimentally.¹³ Calculations employing density-functional theory¹⁴ in Sb/Ge(111) have shown that both $\sqrt{3} \times \sqrt{3}$ and 2×1 phases have the same surface formation energies, slightly lower than the energy for the substitutional 1×1 structure. Recent *ab initio* calculation for this system¹⁵ has also shown that 2×1 chain reconstruction has a range of stability in between 5.5% compression (corresponding to almost Si lattice constant) and 1% expansion, while the 1×1 phase is found stable for larger expansions

and the T_4 - $\sqrt{3} \times \sqrt{3}$ structure for larger compressions.

In general, the formation energies of the $\sqrt{3} \times \sqrt{3}$ and 2×1 phases are very similar in all mentioned 1 ML Sb or Bi covered systems. Extra evidence comes from recent experiment⁴ where small amounts of atomic hydrogen adsorbed on $\sqrt{3} \times \sqrt{3}$ -Sb/Si(111) phase partly reconstruct it into the H- 2×1 -Sb/Si(111). We propose that this reconstruction, as well as high-temperature reconstructions from the $\sqrt{3} \times \sqrt{3}$ and 2×1 phases to disordered phase, could be regarded as phase transitions which are described by the six-state model similar (but not identical) to the six-state Potts model.¹⁶ Moreover, we employ the idea of the structural transition at high temperature from kinetic study⁹ in which strong attractive Sb-Sb interactions were recently found in Sb-Si(111) system when Sb coverage is more than 0.7. Here, we present the description of the six-state model for the 1 ML Sb-Si(111) system, the phase diagram for structural phase transitions from $\sqrt{3} \times \sqrt{3}$ and 2×1 phases to disordered phase, and we also demonstrate how small concentrations of hydrogen can induce experimentally observed 2×1 ordering in the $\sqrt{3} \times \sqrt{3}$ phase.

Denoting the states as shown in Fig. 1, we can write the Hamiltonian (per Sb atom) of the six-state model as consisting of two competing parts: the part responsible for occurrence of the $\sqrt{3} \times \sqrt{3}$ phase trimers (with pair interaction $v_{\sqrt{3} \times \sqrt{3}}$) and the part stimulating occurrence of the zigzag

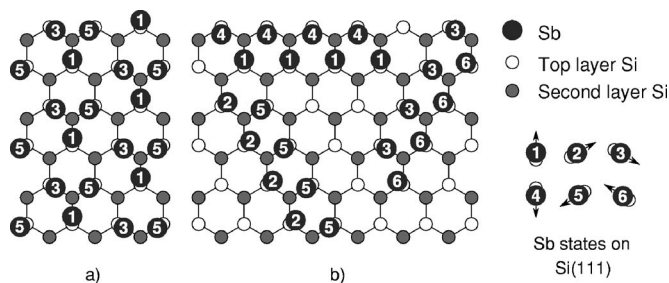


FIG. 1. Schematic representation of $\sqrt{3} \times \sqrt{3}$ phase (a) and fragments of the threefold zigzag 2×1 chains (b) with indicated Sb states (shifts) on Si(111). Arrows and numbers denote the shift of Sb atom from the center of the top layer Si atom.

chains of the 2×1 phase (with pair interaction $v_{2 \times 1}$), i.e., in a form

$$\mathcal{H} = -\frac{1}{2} v_{i,j} \delta(p_i, q_j), \quad (1)$$

where $\delta(p_i, q_j)$ is the Kronecker delta function equal to 1 when combination of states p_i and q_j in the nearest-neighbor (NN) Sb sites i and j corresponds either to $\sqrt{3} \times \sqrt{3}$ or 2×1 phases and zero otherwise, and

$$v_{i,j} = \begin{cases} v_{\sqrt{3} \times \sqrt{3}} & \text{if } (p_i, q_j) = (1,3), (3,5), (5,1) \\ v_{2 \times 1} & \text{if } (p_i, q_j) = (1,4), (2,5), (3,6). \end{cases} \quad (2)$$

In our model, the number of NNs $z=2$, in spite of the coordination number being equal to 6, and both interaction constants are attractive (>0). Three pairs of the $v_{2 \times 1}$ term are due to the fact that 2×1 zigzag chains in hexagonal lattice can run in three possible directions, possessing (1,4), (2,5), and (3,6) states. Calculation of phase transitions with the energy [Eq.(2)] shows that the $\sqrt{3} \times \sqrt{3}$ phase is promoted if $v_{\sqrt{3} \times \sqrt{3}} > v_{2 \times 1}$, but the 2×1 phase is more favorable if $v_{\sqrt{3} \times \sqrt{3}} < v_{2 \times 1}$. *Ab initio* calculations show that NN Sb-Sb bond length on Si and Ge(111) (see Table I) is shorter in the 2×1 than in the $\sqrt{3} \times \sqrt{3}$ phase. We assume that this indicates stronger attraction for $v_{2 \times 1}$ leading to inequality $v_{2 \times 1} \geq v_{\sqrt{3} \times \sqrt{3}}$ and occurrence of the 2×1 phase. This contradicts recent data⁴ claiming that in most cases the $\sqrt{3} \times \sqrt{3}$ phase, sometimes with small inserts of the 2×1 phase, is observed in experiments. The contradiction could be resolved easily by considering the effect of triple interactions in $\sqrt{3} \times \sqrt{3}$ trimer or assuming that the site binding energy ϵ , for the states absent in trimers but existing in the zigzag chains, is a bit higher, i.e., by adding the following terms to the energy [Eq. (1)]: $-\frac{1}{3} v_t \delta(p_i, q_j, r_k) + \epsilon [\delta(2, q_i) + \delta(4, q_i) + \delta(6, q_i)]$. Here, $v_t > 0$, $\epsilon > 0$, and the states of a trimer contribute only if $p_i, q_j, r_k = 1, 3, 5$, i.e., only for the $\sqrt{3} \times \sqrt{3}$ phase. It should be noted that consideration of the triple interactions and inequality $v_{2 \times 1} \geq v_{\sqrt{3} \times \sqrt{3}}$ are essential for our model to describe

TABLE I. NN distance d between adsorbates in 1 ML covered phases.

d	$\sqrt{3} \times \sqrt{3}$ phase	2×1 phase	References
Sb-Sb on Si(111)	2.89 Å	2.8 Å	<i>ab initio</i> ^a
	2.81 Å		<i>ab initio</i> ^b
	2.87 ± 0.02 Å		SEXAFS ^c
		3.1 Å	STM ^d
Sb-Sb on Ge(111)	2.9 ^e	2.85 Å	<i>ab initio</i> ^f
		2.86 ± 0.03 Å	SEXAFS ^g
	2.87 Å	2.82 Å	<i>ab initio</i> ^h
Bi-Bi on Si(111)	3.1 Å		<i>ab initio</i> ⁱ

^aReference 7.

^bReference 8.

^cSurface extended x-ray adsorption fine structure (Ref. 2).

^dReference 6.

^eCorrected in Ref. 7.

^fReference 14.

^gReference 13.

^hReference 15.

ⁱReference 12.

hydrogen-induced $\sqrt{3} \times \sqrt{3} \rightarrow 2 \times 1$ reconstruction. Further, for calculations, we use hexagonal lattice of 48×48 Sb sites, take $v_t = v_{\sqrt{3} \times \sqrt{3}}$, and neglect the effect of site binding energy ($\epsilon=0$).

Phase diagrams of the model [Eq. (1)], calculated by Monte Carlo method using Metropolis algorithm for different values of the ratio $v_{2 \times 1}/v_{\sqrt{3} \times \sqrt{3}}$ without and with the term of triple interaction, are presented in Figs. 2(a) and 2(b), respectively. The phase transitions from both ordered phases ($\sqrt{3} \times \sqrt{3}$ and 2×1) to disordered phase (with probability of each state approximately equal to 1/6) are calculated. The phase transition temperature T_c is determined from the peak of temperature dependence of specific heat.

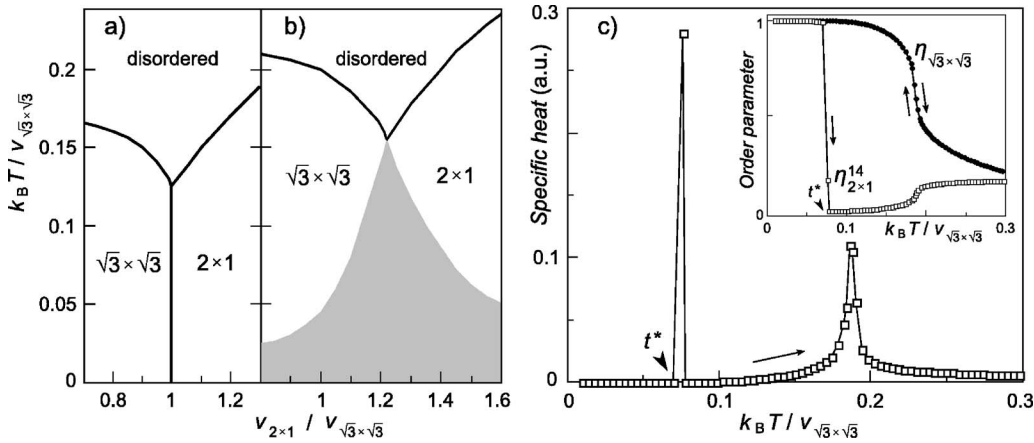


FIG. 2. Phase diagram at (a) $v_t=0$ and (b) $v_t/v_{\sqrt{3} \times \sqrt{3}}=1$. Solid lines denote order-disorder phase transition temperature T_c . Shaded region corresponds to mixed state. (c) Temperature dependences of specific heat and order parameters (inset) at $v_{2 \times 1}/v_{\sqrt{3} \times \sqrt{3}}=1.1$ and $v_t/v_{\sqrt{3} \times \sqrt{3}}=1$. Results shown by open squares are obtained simulating from low temperature and perfect 2×1 [(1,4) chains] phase inside the area of the $\sqrt{3} \times \sqrt{3}$ phase. The denotation $t^* = k_B T^*/v_{\sqrt{3} \times \sqrt{3}}$ is for the transition point from pure to mixed state (k_B —Boltzmann constant). Solid circles in the inset denote T dependence of $\sqrt{3} \times \sqrt{3}$ phase order parameter (note the absence of hysteresis).

When $v_t=0$, the triple point of coexistence of all three phases is at $v_{\sqrt{3}\times\sqrt{3}}=v_{2\times 1}$, and the boundary between $\sqrt{3}\times\sqrt{3}$ and 2×1 phases continues from this point down to zero temperature [see Fig. 2(a)]. The phase transitions to disordered phase are of the second order. In specific heat and order parameter dependences on temperature, we did not notice any hysteresis, which usually indicates first-order nature of the transitions. This might mean that such type of transitions does not belong to Potts model universality class, since phase transitions of the six-state Potts model are of the first order.

The transitions with included v_t term are more complicated [see Fig. 2(b)]. The triple point is found at $v_{\sqrt{3}\times\sqrt{3}}+2v_t/9=v_{2\times 1}$, instead of the point $v_{\sqrt{3}\times\sqrt{3}}+v_t/3=v_{2\times 1}$ which follows from the ground-state ($T=0$) analysis. This result implies that close to the $v_{\sqrt{3}\times\sqrt{3}}+v_t/3=v_{2\times 1}$ boundary, the phase transitions are of the first order and separation of both phases takes place. Calculations starting from the disordered phase at every temperature step showed the second-order phase transition between a disordered phase and one of the ordered phases without any hysteresis and phase separation at $T<T_c$ [see the behavior of the order parameter $\eta_{\sqrt{3}\times\sqrt{3}}=\langle\delta(1,3,5)\rangle$ at decreasing T , Fig. 2(c)]. To find the boundaries of the mixed or metastable state region, we performed the calculations by increasing temperature from very low T starting from perfectly ordered 2×1 structure [(1, 4) chains] inside the $\sqrt{3}\times\sqrt{3}$ region in the phase diagram. The 2×1 phase is not instantly rearranged into the $\sqrt{3}\times\sqrt{3}$, but remains intact with increase in temperature, and only at higher temperature point T^* (indicating the loss of metastability or end of two-phase $\sqrt{3}\times\sqrt{3}+2\times 1$ region) transits to the $\sqrt{3}\times\sqrt{3}$ phase. This transition is followed by the transition to the disordered phase at $T_c>T^*$ [see temperature dependence of specific heat and order parameter $\eta_{2\times 1}^{14}=\langle\delta(1,4)\rangle$, Fig. 2(c)]. Actually, it might indicate that the free energy of the system close to the $\sqrt{3}\times\sqrt{3}$ and 2×1 phase boundary has two minima corresponding to both these phases, and one of these minima (that of the 2×1 phase) decreases with increase in T and disappears at the metastability limit point T^* . The pure $\sqrt{3}\times\sqrt{3}$ phase exists between T^* and T_c .

Similar results are obtained when we start calculations from the perfect $\sqrt{3}\times\sqrt{3}$ structure inside the 2×1 region of the phase diagram. In this case, the minimum corresponding to the $\sqrt{3}\times\sqrt{3}$ phase disappears at T^* . Immobility of Sb atoms in our simulations due to low temperature can be ruled out, since the boundary of the mixed region [$T^*(v_{2\times 1}/v_{\sqrt{3}\times\sqrt{3}})$] is clearly shown to depend on $v_{2\times 1}/v_{\sqrt{3}\times\sqrt{3}}$. Special Monte Carlo methods should be employed to obtain the order of transitions near the $\sqrt{3}\times\sqrt{3}\rightarrow 2\times 1$ phase boundary. However, we doubt if such simulations would be expedient until these transitions were confirmed by experimental data.

The kinetic study⁹ can be reinterpreted in terms of our model providing us with approximate temperature of the structural order-disorder phase transition. By plotting adsorption isotherms at different temperatures, the value of NN Sb-Sb attractive lateral interaction $V_{\text{Sb-Sb}}=0.08$ eV was obtained in this work when Sb coverage in Sb-Si(111) exceeds 0.7 ML. The two-dimensional (2D) condensation in Sb overlayer was assumed, and the value of a critical temperature of the structural transition, $T_c=870$ K, was estimated using lattice-gas model in mean-field approximation (MFA). In spite of the attractive interactions, no first-order transitions were expected.

The number of NNs in Ref. 9 was $z=6$ as usual for hexagonal lattice when Sb atoms occupy either on top or fcc or hcp sites. Therefore, $zV_{\text{Sb-Sb}}=0.48$ eV. In our model, when Sb atom in both ordered phases is closer to 2, but further from the remaining four neighbors, $z=2$. Thus, for our model $V_{\text{Sb-Sb}}=0.24$. At $v_t/v_{\sqrt{3}\times\sqrt{3}}=1$ and close to the $\sqrt{3}\times\sqrt{3}\rightarrow 2\times 1$ phase boundary and the triple point, we obtain from the phase diagram $k_B T_c/v_{\sqrt{3}\times\sqrt{3}}=0.155$ and $v_{\sqrt{3}\times\sqrt{3}}=2V_{\text{Sb-Sb}}=0.48$ eV because of coefficient of $\frac{1}{2}$ used by us before interaction constant in Hamiltonian [Eq. (1)]. Substituting the value of $v_{\sqrt{3}\times\sqrt{3}}$, we obtain $T_c\approx 870$ K. It should be noted that a variation of trimer interaction v_t does not change T_c considerably, e.g., for very low v_t , $k_B T_c/v_{\sqrt{3}\times\sqrt{3}}=0.13$, and $T_c\approx 730$ K.

It is also interesting to compare the phase transition temperature obtained by our model with the MFA results of 2-dimensional q -state Potts model. The result for $q=6$ and

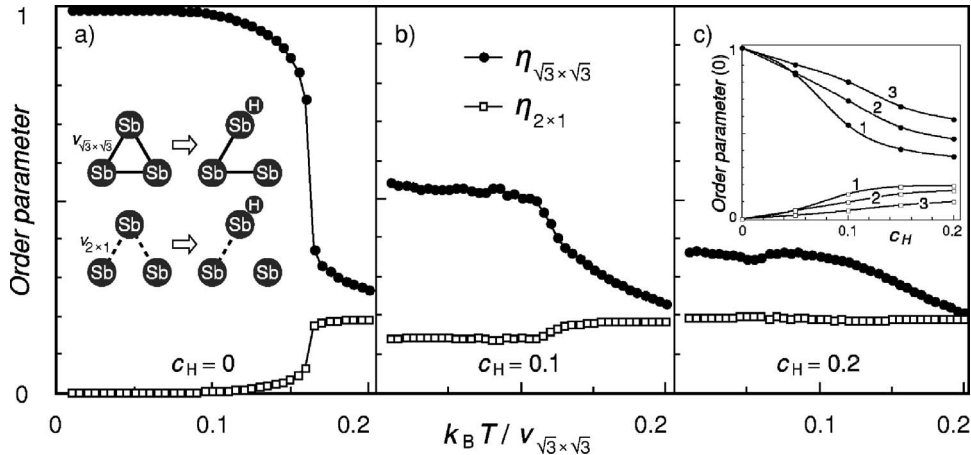


FIG. 3. Temperature dependences of order parameters $\eta_{\sqrt{3}\times\sqrt{3}}$ and $\eta_{2\times 1}$ at $v_{2\times 1}/v_{\sqrt{3}\times\sqrt{3}}=1.21$ and hydrogen coverage c_H =(a) 0, (b) 0.1, and (c) 0.2. Inset in (a): schematic representation of hydrogen atom breaking randomly one of two Sb-Sb bonds and canceling interaction constant on that bond. Inset in (c): dependence of order parameters $\eta_{\sqrt{3}\times\sqrt{3}}$ and $\eta_{2\times 1}$ at $T\rightarrow 0$ on c_H for different distances from the phase boundary [$v_{2\times 1}/v_{\sqrt{3}\times\sqrt{3}}=(1) 1.21, (2) 1.15, \text{ and } (3) 0.99$]. 113308-3

$z=2$ yields $k_B T_c / v_{NN} \approx 0.5$ for the first-order phase transition and $k_B T_c / v_{NN} \approx 0.33$ for the (nonexisting) second-order phase transition.¹⁶ Thus, the result of our model (at $v_{\sqrt{3} \times \sqrt{3}} = 2v_{NN}$) is very close to the lower, second-order phase transition of the Potts model.

Adsorption of hydrogen atoms changes the structure of Sb overlayer on Si(111). Instead of the perfect $\sqrt{3} \times \sqrt{3}$ phase, large areas of the zigzag chains corresponding to the 2×1 pattern are found.⁴ In model (1), we distribute hydrogen atoms randomly in the $\sqrt{3} \times \sqrt{3}$ structure. The interaction parameters are chosen in the $\sqrt{3} \times \sqrt{3}$ part of the phase diagram of Fig. 2(b), but very close to the $\sqrt{3} \times \sqrt{3} \rightarrow 2 \times 1$ phase boundary. This choice is justified, since both phases have the same surface formation energy.⁷ We assume that a hydrogen atom randomly breaks off one of two Sb-Sb bonds when adsorbed close to (on) Sb atom, as shown in the inset of Fig. 3(a). Then, H atom cancels the interaction corresponding to the broken bond. If the broken bond belongs to $\sqrt{3} \times \sqrt{3}$ trimer, the local energy increases by $v_{\sqrt{3} \times \sqrt{3}} + v_t/3$, and the two remaining $v_{\sqrt{3} \times \sqrt{3}}$ interactions of the trimer can be readily substituted by $v_{2 \times 1}$ interaction promoting the 2×1 ordering, if $v_{2 \times 1} > v_{\sqrt{3} \times \sqrt{3}}$.

In such manner, part of trimers can be substituted by zigzag chains running in one, two, or three directions. In our simulations, this is demonstrated by temperature dependences of order parameters $\eta_{\sqrt{3} \times \sqrt{3}}$ and $\eta_{2 \times 1} = \frac{1}{3}[\langle \delta(1,4) \rangle + \langle \delta(2,5) \rangle + \langle \delta(3,6) \rangle]$ (Fig. 3) and low-temperature snapshot (Fig. 4). Insertion of hydrogen atoms decreases the T_c of disordered-to- $\sqrt{3} \times \sqrt{3}$ transition, weakening and smoothing the anomalies of functions characterizing this point. The length and number of zigzag chains grows with an increase in hydrogen concentration c_H . At low c_H (< 0.05), trimers possessing H atom loose one bond, but no chains with more than three Sb atoms are created. When $c_H = 0.1$, a large part of H atoms are located at (or very close to) the ends of small chains. This might be seen in the snapshot of our simulation. When c_H is around 0.2, a part of H atoms finds itself comfortable even inside the chains as well. Actually, hydrogen

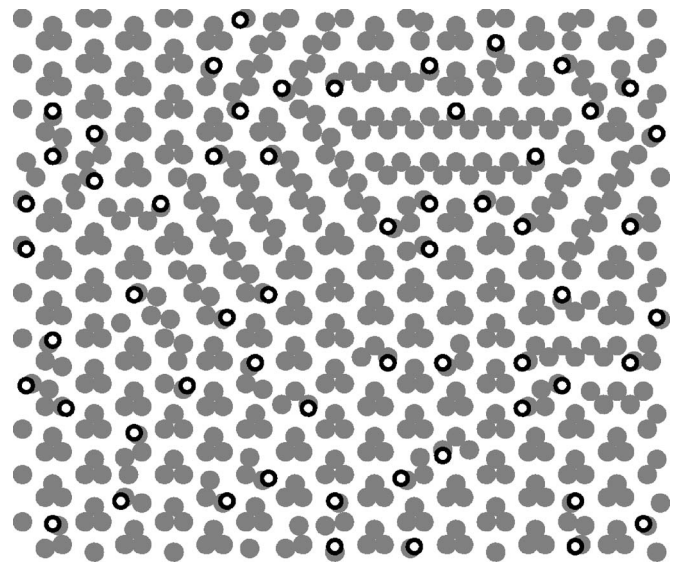


FIG. 4. The snapshot of our simulation at $c_H = 0.1$, $v_{2 \times 1} / v_{\sqrt{3} \times \sqrt{3}} = 1.21$, and $k_B T / v_{\sqrt{3} \times \sqrt{3}} = 0.1$. Gray circles—Sb atoms and small white circles—H atoms.

atoms force the zigzag chains to “freeze” inside the $\sqrt{3} \times \sqrt{3}$ environment keeping the chains “pinned” by the H atoms. Our model is perfectly suited to explain the experimental data,⁴ since a similar scheme of H-induced $\sqrt{3} \times \sqrt{3} \rightarrow 2 \times 1$ reconstruction was recently suggested in Ref. 4.

In conclusion, our simulations imply that the phase transitions from disordered to both ordered phases are of the second order, though at lower temperature, phase separation might be expected if triple interaction is taken into account. In case of hydrogen adsorption, hydrogen-induced trimer to zigzag chains reconstruction is readily obtained using our model.

We are grateful to S. Lapinskas for a number of valuable discussions. This work was supported by the Lithuanian State Science Foundation and EC project PRAMA.

¹C. Y. Park, T. Abukawa, T. Kinoshita, Y. Enta, and S. Kono, Jpn. J. Phys. **27**, 147 (1988).

²J. C. Woicik, T. Kendelewicz, K. E. Miyano, P. L. Cowan, C. E. Bouldin, B. A. Karlin, P. Pianetta, and W. E. Spicer, Phys. Rev. B **44**, 3475 (1991).

³P. Mårtensson, G. Meyer, N. M. Amer, E. Kaxiras, and K. C. Pandey, Phys. Rev. B **42**, 7230 (1990).

⁴O. Kubo, T. Fujino, J.-T. Ryu, K. Oura, and M. Katayama, Surf. Sci. **581**, 17 (2005).

⁵Vinod Kumar Paliwal, A. G. Vedeshwar, and S. M. Shivaprasad, Phys. Rev. B **66**, 245404 (2002).

⁶H. B. Elswijk, D. Dijkkamp, and E. J. van Loenen, Phys. Rev. B **44**, 3802 (1991).

⁷N. Takeuchi, J. Vac. Sci. Technol. A **16**, 1790 (1998).

⁸E. Kaxiras, Europhys. Lett. **21**, 685 (1993).

⁹H. Guesmi, L. Lapena, A. Ranguis, P. Müller, and G. Tréglia,

Phys. Rev. Lett. **94**, 076101 (2005).

¹⁰R. Shioda, A. Kawazu, A. A. Baski, C. F. Quate, and J. Nogami, Phys. Rev. B **48**, 4895 (1993); S. Nakatani, T. Takahashi, Y. Kuwahara, and M. Aono, *ibid.* **52**, R8711 (1995).

¹¹J. M. Roesler, T. Miller, and T.-C. Chiang, Surf. Sci. **417**, L1143 (1998).

¹²T. M. Schmidt, R. H. Miwa, and G. P. Srivastava, Braz. J. Phys. **34**, 629 (2004).

¹³T. Kendelewicz, J. C. Woicik, K. E. Miyano, S. A. Yoshikawa, P. Pianetta, and W. E. Spicer, J. Vac. Sci. Technol. A **12**, 1843 (1994).

¹⁴N. Takeuchi, Phys. Rev. B **53**, 7996 (1996).

¹⁵A. Antons, Y. Cao, B. Voigtländer, K. Schroeder, R. Berger, and S. Blgel, Europhys. Lett. **62**, 547 (2003).

¹⁶F. Y. Wu, Rev. Mod. Phys. **54**, 235 (1982).